Identifying the Statistically-Most-Concerning Conjunctions in LEO

Matthew Stevenson
LeoLabs
Darren McKnight
LeoLabs
Hugh Lewis
University of Southampton
Chris Kunstadter
AXA XL
Rachit Bhatia
LeoLabs

ABSTRACT

The mapping of all close approaches in low Earth orbit (LEO) by collision probability, consequence, and risk provides insight into both current and future collision hazards. Probability is determined using the miss distance, hard body radius, and covariance derived from the LeoLabs data platform. Consequence is calculated using the mass involved in the event (which in turn represents the amount of debris likely produced if a collision were to occur). Monitoring the ensemble of LeoLabs-collected conjunction data identifies the statistically-most-concerning events in the past year in two families of events: (1) between operational satellites and all objects and (2) among debris objects, including fragments and massive derelict objects. Close approaches in the first group represent space traffic management concerns, while those in the second group can only be managed through debris remediation. The conjunction data is parsed by object name, type, altitude, risk, and country of origin. This analysis highlights the criticality of looking at collision risk holistically by altitude and types of objects involved in these conjunctions to identify priorities for controlling debris growth in the future.

1. INTRODUCTION

Use of low Earth orbit (LEO) is increasing in both intensity and diversity – more countries are operating a wide variety of satellites in LEO, and the promise of large constellations is being realized. While this bodes well for the space industry it poses a challenge in determining the balance of regulation and incentivization that is needed to keep space activity safe and vibrant. On one hand, it is imprudent to discourage the evolution of the space enterprise, however, regulation must be sufficient to allow reliable operations, free from collision hazard and associated risks (such as risk to aviation and ground assets from reentering space hardware). Unfortunately, there are many factors that affect assessing the most effective ways to enhance space safety, ensure long-term operational efficiencies, and promote future system deployments.

Debris-generating potential is proposed as the most important feature to scrutinize in LEO, as it is a leading indicator for future concerns for both trackable debris (which drives collision avoidance burden and further debris-generating events) and lethal nontrackable (LNT) debris (which drives mission-terminating collision hazard). This paper will examine these issues in two parts. First, the LEO Collision Risk Continuum (LCRC) [1] is updated using a full year's worth of conjunction data messages (CDMs) to determine the objects and orbits that pose the greatest debris-generating potential. Second, a model is developed that suggests an orbital capacity measure to further refine the concept of identifying the regions and objects in LEO that require the most scrutiny to achieve space operations assurance. Our analysis has led us to conclude that constellations in LEO may indeed not be the primary cause for future debris growth concerns but will rather be the victims of decades of a *laissez-faire* attitude regarding debris mitigation and remediation. More pointedly, the actual mathematics previously used to characterize collision risk may have to be re-thought as constellations of small, nimble, and capable satellites in large constellations may have their collision risk poorly estimated by simply examining an aggregate probability of collision (PoC) threshold, particularly among members of a well-orchestrated constellation.

2. LCRC UPDATE

The LCRC has been created for the period of 1 July 2020 to 30 June 2021. All of the plots are identical to the original LCRC development [1] except for the following aspects:

- Internal conjunctions for the Starlink constellation are omitted from the LCRC plot (i.e., removed from the OPL-ALL) since they pose negligible debris-generating potential due to the robust operational stationkeeping and collision avoidance capability exhibited to date; the number of these events are noted for context.
- Conjunctions with the ISS only consider the consequence to be two times the impactor mass and do not consider the entire mass of the ISS. Note that a collision between the ISS and a trackable object might cause loss of life – we consider this to be very serious, but our analysis is focused solely on the debris-generating consequence of high-risk conjunctions.

Before examining the LCRC plots, the spatial density and mass distribution plots for LEO as of 1 July 2021 are provided in Figures 1 through 4. Figure 1 plots the number of objects per cubic kilometer as a function of altitude and type of object, while Figure 2 shows the percentage of each type of object as a function of altitude. These figures highlight that, at most altitudes in LEO, fragmentation debris is the prevalent type of object by number. However, there are spikes of operational satellites that clearly depict satellite constellations such as Planet, Starlink, Iridium, OneWeb, Gonets, Globalstar, and others.

Figures 3 and 4 show that the number of objects in LEO only provides part of the story. When the mass of the cataloged objects is plotted, the contribution of the intact derelict objects (i.e., rocket bodies and payloads) becomes apparent. Since these massive objects have no ability to avoid collisions amongst themselves or operational payloads, this creates a significant debris-generating potential. The log mass density shows that nonoperational payloads and rocket bodies dwarf the mass from operational payloads in all altitudes except below 550 km and around 1200 km and 1500 km. In addition, the mass percentage plot in Figure 4 shows that the rocket bodies contribute much more to the total mass than the nonoperational payloads because of their larger average mass (~1,500 kg vs ~1,000 kg for payloads). Lastly, the high mass density near operational satellites identifies regions of particular concern, as debris from collisions will immediately spread over hundreds of kilometers in altitude, especially for LNT debris of 1 to 10 cm in size.

These plots provide valuable context for the generation of the LCRC plots: (1) massive derelicts comprise the majority of the mass in most LEO orbits; (2) fragmentation debris is the most populous component of the LEO population at most altitudes; (3) operational payloads dominate at a few altitudes in LEO where significant constellations have been deployed; and (4) growing constellations are adjacent to or overlap altitudes of high debris-generating potential from massive derelict objects.

The LCRC is generated with the following definitions and assumptions:

- The PoC is taken from the LeoLabs data platform. All conjunctions with a PoC > 1E-6 are used.
- The consequence for each event is the total mass of the objects (in kg) involved in a potential collision. This is a surrogate for the amount of debris that would likely be produced if a collision occurs.
- The risk is simply the product of the PoC and the consequence (mass). This “risk” has units of kg and is proportional to the projected number of debris fragments. A good rule of thumb is that the number of cataloged fragments from a catastrophic collision is 2 to 3 times the mass involved in the collision; the number of LNT produced is about ten times more numerous than the cataloged fragments.
- There are two families of conjunctions plotted: (1) operational payloads (OPL) against all objects (i.e., OPL-ALL), including OPL-OPL and OPL-DEB, with DEB being fragments from collisions and breakups (FRAG) and intact massive derelict (MD) rocket bodies (R/B) and payloads (PL); and (2) collisions between two debris objects (DEB-DEB).
- For this exercise, the LeoLabs catalog had 16,852 objects as of June 30, 2021, of which 2,555 were OPL.
- The resulting risk values are plotted with equal risk contours to differentiate the groupings of conjunctions.
- The risk values for all conjunctions are then plotted as a function of altitude.
- The aggregate risk of these conjunctions is calculated by adding all the contributions for each altitude to depict the total debris-generating potential as a function of altitude.

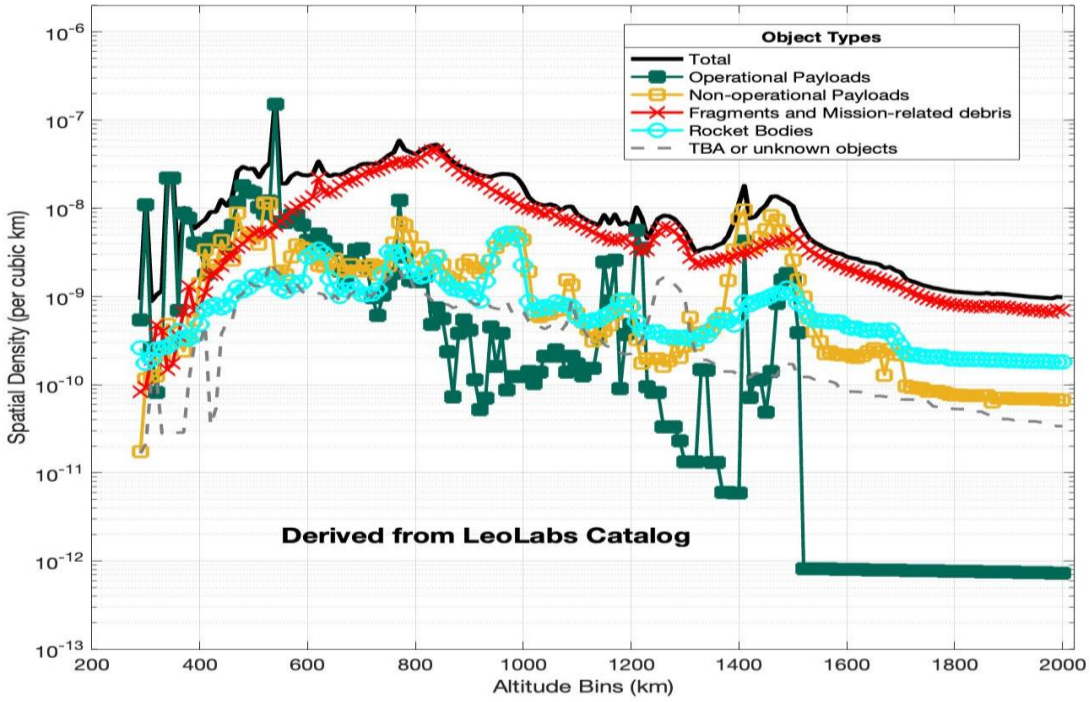

Fig. 1. Spatial density (SPD = number of objects per km^3) shows that, at almost all altitudes in LEO, operational payloads are outnumbered by debris (either fragments or intact derelict objects). Below ~550 km and at 1,200 km and 1,400 km, operational payloads exceed fragmentation debris.

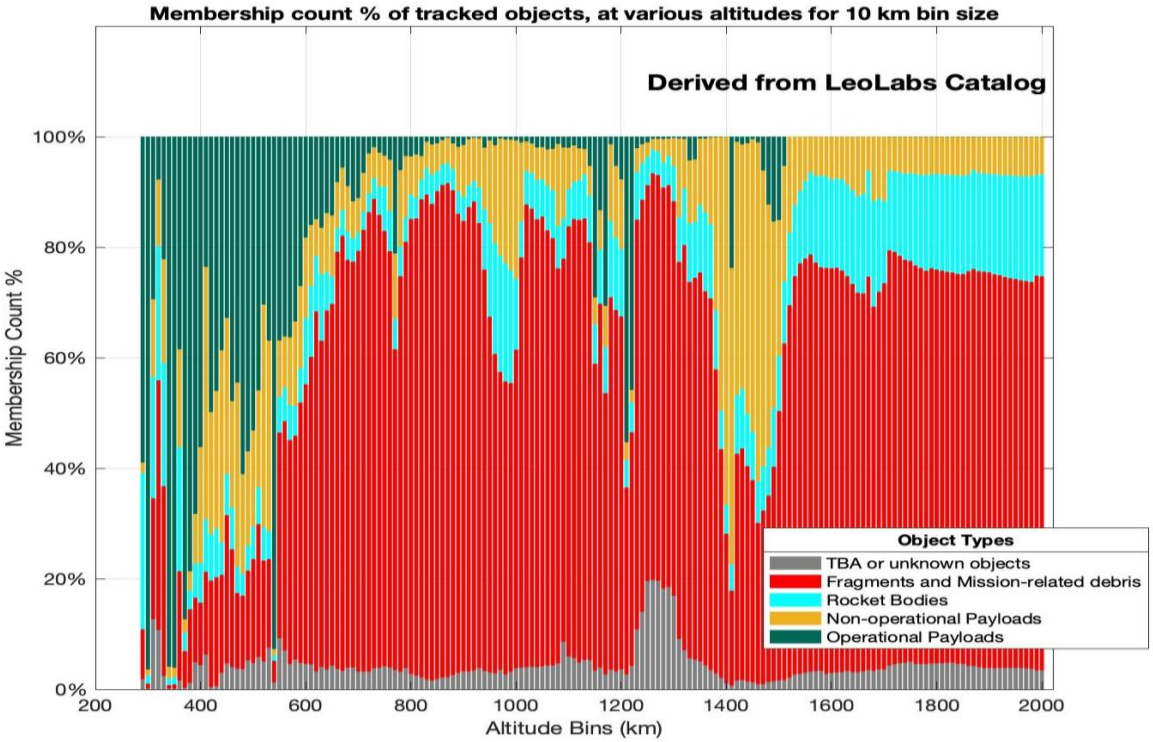

Fig. 2. The membership count % (by object type) shows how the mix of objects below 500 km varies considerably by altitude bin, but between 500 and 800 km there are several obvious spikes in operational satellites that represent satellite constellations.

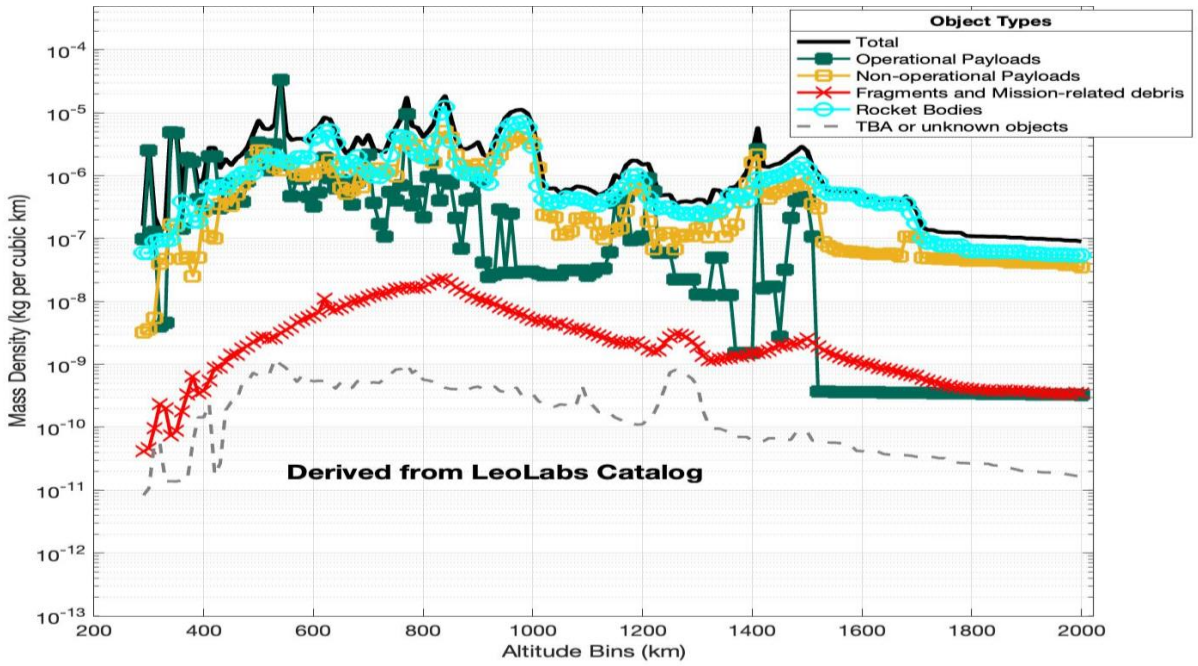

Fig. 3. The mass density distribution (log scale) in LEO highlights that massive derelicts drive the mass at most altitudes.

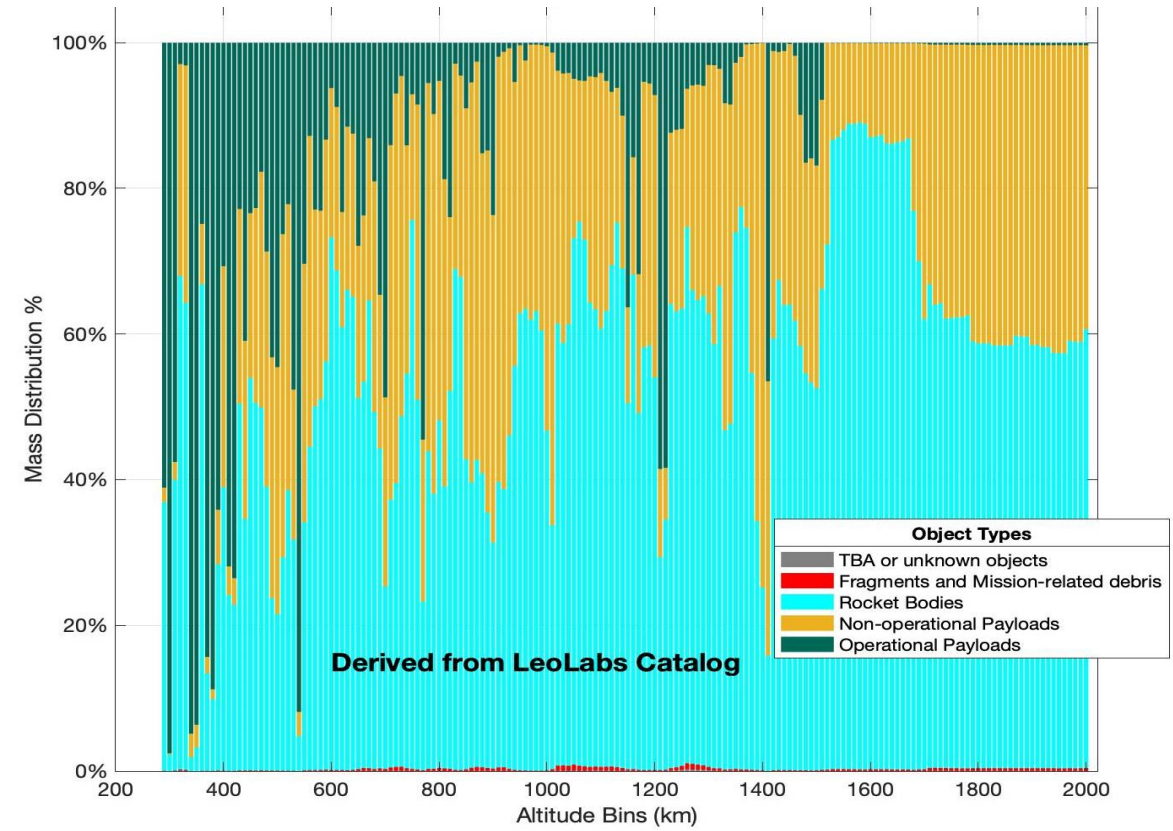

Fig. 4. Mass distribution by percentage in LEO further amplifies the contribution of abandoned rocket bodies and nonoperational payloads to the resident mass on orbit except in a few specific altitudes.

Figure 5 shows the LCRC with the risk regions as defined previously. Risk is greatest in Region I and decreases towards Region VI. The total number of conjunctions logged by LeoLabs was 1,430,996, however, 670,025 (over 45% of all conjunctions) were not plotted since they were "internal" conjunctions for Starlink – we assume that close encounters at high relative velocities between operational satellites within a well-maintained constellation do not pose a meaningful collision risk. There were no significant "internal" conjunctions for other constellations. Figure 5 shows a total of 760,971 conjunctions representing over 63,000 per month. Appendix A lists the top 30 conjunctions of the 760,971 depicted.

The overall shape of the two families of conjunction events (OPL-ALL and DEB-DEB) are similar, with both showing some clear families of consequences (represented by horizontal lines) from many objects of a similar mass in many of the conjunctions. The most pronounced high-consequence events (horizontal orange line extending from ~10^4 mass) are caused by SL-16 rocket bodies primarily residing in the 830 to 850 km altitude region.

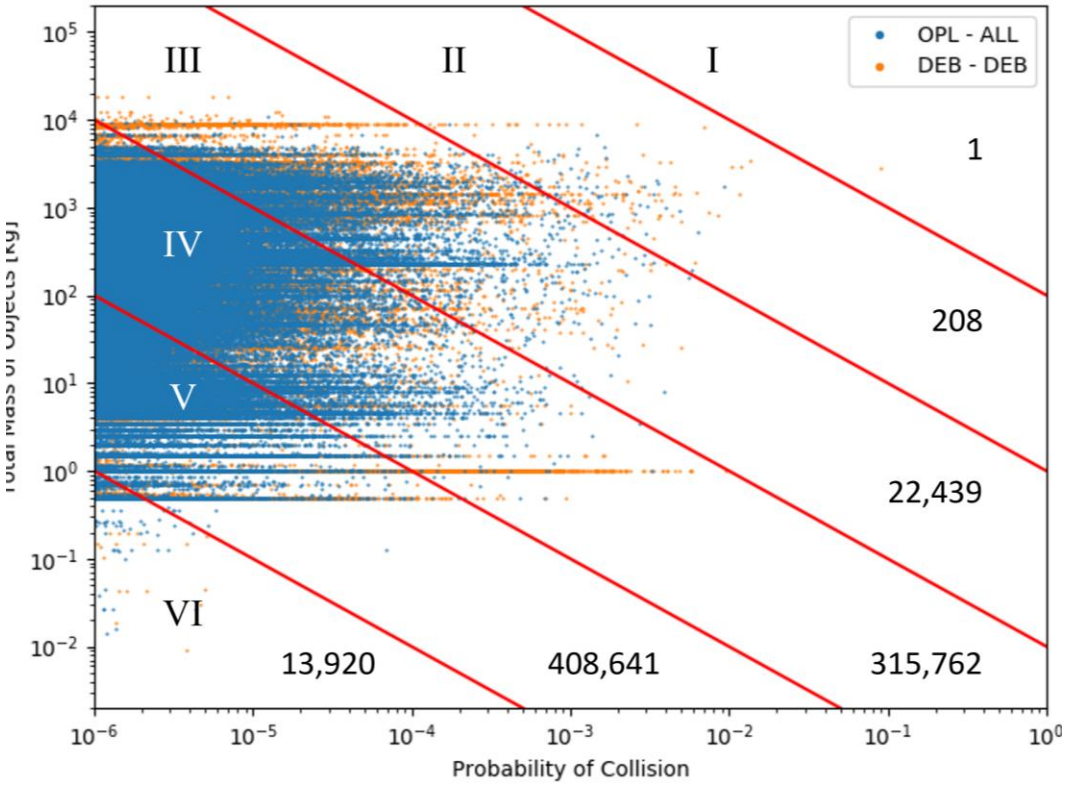

Fig. 5. The LCRC graphically displays the debris-generating potential in two families: (1) OPL-ALL represents risks that can be mitigated through space traffic management, while (2) DEB-DEB represents the existing debris-generating potential that can only be managed through debris remediation.

Figure 6 provides the LCRC with the two families of conjunctions separated to allow closer scrutiny of these distributions. As in the previous analysis, DEB-DEB contributes the most to all risk regions except for the middle risk region. DEB-DEB comprises 65% of all events in the top two risk regions (136 out of 209 conjunctions), 62% in top three risk regions, and 88% of the lower two risk regions. The massive derelicts drive the high-end risk and the debris fragments the low-end risk. In risk region IV, OPL-ALL conjunctions account for 64% of all conjunctions; this is the only region where OPL-ALL surpasses DEB-DEB events.

Figure 7 plots the conjunctions as a function of altitude, with the spikes in OPL-ALL representing constellations and spikes in DEB-DEB corresponding to clusters of massive derelicts. The low-consequence "haze" from the DEB-DEB events represents the potential collisions with the fragment population.

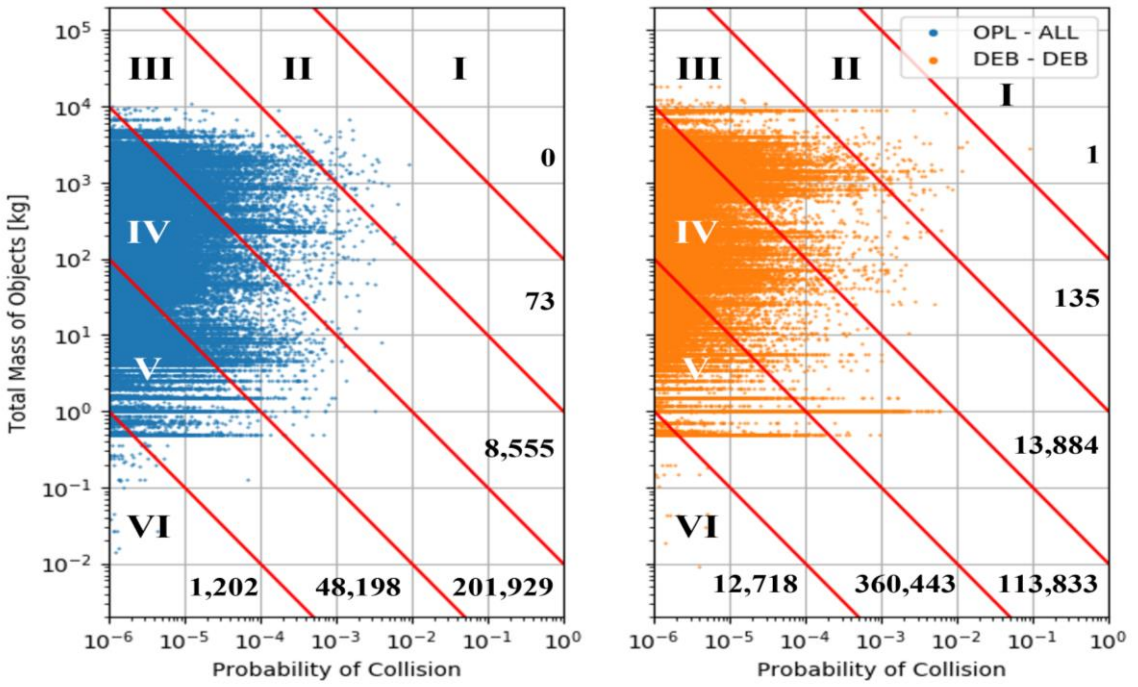

Fig. 6. By separating the two families of conjunctions, the greater contribution from DEB-DEB is clear; DEB-DEB events comprise 62% of the conjunctions in the top three risk regions and 65% in the top two risk regions.

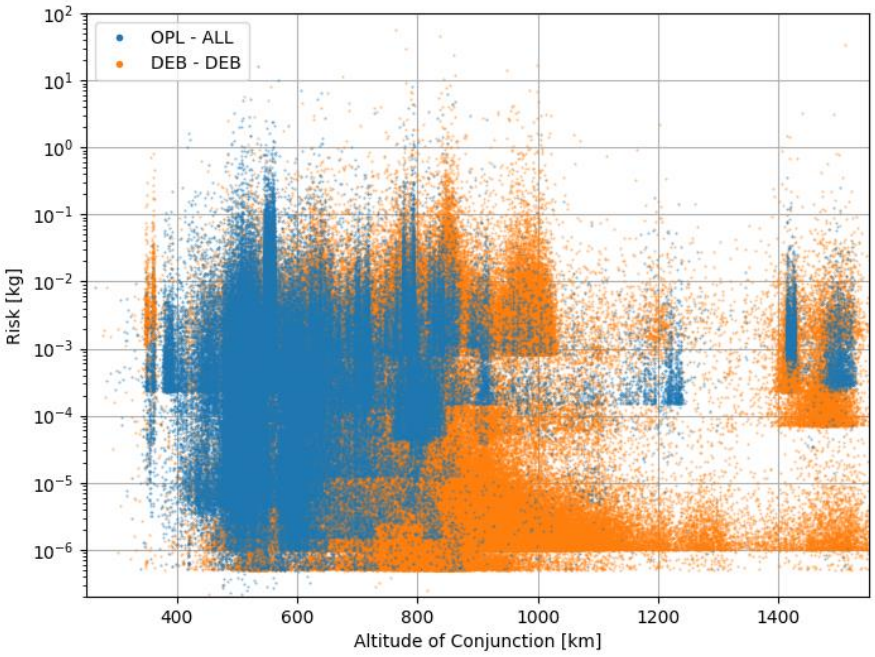

Fig. 7. Plotting the data from the ~760,000 CDMs as a function of altitude provides a spatial depiction of debris-generating potential, highlighting both constellations of operational satellites and clusters of massive derelict objects. The haze in the lower third of the figure represents the collision hazard from debris fragments.

Figure 8 aggregates the risk values as a function of altitude, highlighting that the debris-generating potential in LEO is driven by massive derelicts colliding with each other rather than operational satellites' ability to avoid catastrophic collisions. The only region where STM concerns (OPL-ALL) are larger than debris remediation issues (DEB-DEB) is between 400 and 550 km, peaking just above 500 km, largely due to the Starlink constellation. Even where OPL-ALL is greater than DEB-DEB, it should be noted that this risk is likely less than depicted since use of high accuracy ephemeris by operational satellites may reduce the probability (due to a smaller position covariance), and, thus, the actual risk of many of the OPL-ALL conjunction events.

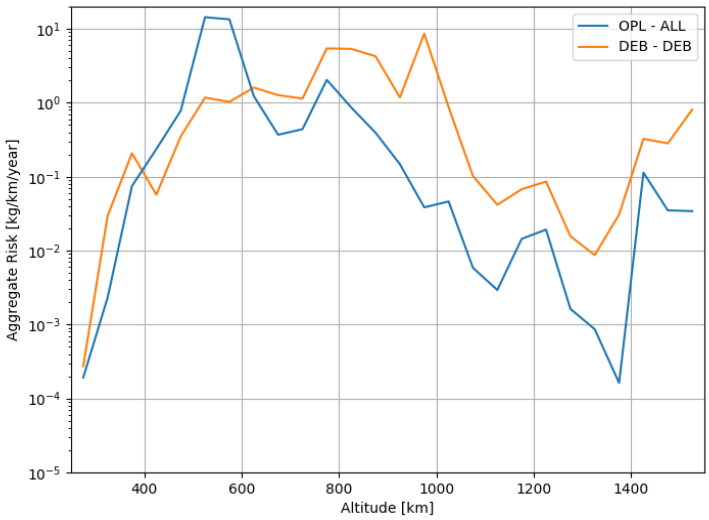

Fig. 8. The only region where STM risks are greater than derelict collisions is in the vicinity of the Starlink constellation. Luckily, this risk is mitigated to a great extent through collision avoidance operations and high accuracy ephemeris of the Starlink satellites. Note that this figure is truncated at 1,500 km since, for much of the last year, objects above 1,500 km were not tracked regularly by four of the six LeoLabs radars.

The top 200 conjunctions that pose the greatest debris-generating risk in LEO have been extracted from the ~760,000 conjunctions for closer examination. 65% of these events were DEB-DEB while only 35% were OPL-ALL, as these top 200 conjunctions map almost exactly to the 209 conjunctions in the top two risk regions. Of the 400 objects involved in the 200 events over 50% were intact derelict objects, nearly 30% were debris fragments, and fewer than 20% were operational payloads. Nearly half of the events (96 out of 200) involved a massive derelict object and a fragment, while two massive derelict objects were involved 36 times (18% of the events) and an operational payload encountered a massive derelict 44 times (22% of the 200 events).

In previous examinations of the statistically-most-concerning objects in LEO, Russian rocket bodies have been prominent [3-5]. This evaluation resulted in a similar finding, with the following number of objects (out of 400) appearing in each category:

- Russia had 205 objects: 77 Russian rocket bodies – 35 SL-8, 21 SL-16, 10 SL-3, 10 SL-14, and 1 SL-12; including 3 occurrences of SL-8-on-SL-8 conjunctions; 8 operational payloads; 90 nonoperational payloads; and 30 fragments from Russian breakups – 12 from C1275, 10 from C2251, 6 from SL-16, 1 from Cosmos 375, and 1 from Cosmos 1814.
- The US had 114 objects: 40 operational payloads; 55 massive derelicts – 4 rocket bodies and 51 payloads; and l9 fragments (12 from THOR AGENA D R/B, 4 from NOAA 16, 2 from Iridium 33, and 1 from Scout A).
- China had 63 objects: 27 payloads – 11 operational and 16 nonoperational; 9 rocket bodies; and 27 fragments – 26 from Fengyun-1C and 1 from CZ-4.

It should be noted that the 400 objects represent a wide variety of countries: 50% Russian, 28% US, 16% Chinese, 2% European, 1% Japan, 1% India, and 2% Other. This is a smaller ratio for Russia than in previous analyses, but they still account for about half of the debris-generating potential. It is noteworthy that Iridium 33 debris poses little hazard in comparison to Cosmos 2251 and Fengyun-1C debris; Iridium 33 debris has been affected much more by atmospheric drag than debris from the other two events largely due to different material construction of the spacecraft.

The four individual objects that showed up most often were Russian massive derelict objects launched between 1984 and 1992 – each showed up three times:

- Cosmos 1536 at ~549 km
- Cosmos 1378 at ~495 km
- SL-16 R/B (SSN 22285) at ~842 km
- SL-16 R/B (SSN 23088) at ~843 km

Examining the distribution of these events by altitude shows that 2/3rds of the events occurred between 705 and 1035 km, with the peak activity around ~850 km. Nearly 40 events (~20%) occurred between 485 and 595 km; with 28 of these involving operational payloads – a much greater percentage (70%) than for any other altitude. Notably, despite Starlink having the vast majority of the operational satellites in LEO, there were only ten occurrences of Starlink satellites being involved in the top 200 most-concerning conjunctions. This reinforces that remediation of massive derelict objects provides greater benefit than micro-managing large constellations of agile smallsats. More specifically, Starlink satellites account for about 10% of the LEO population but only 2.5% (10) of the 400 objects in the top 200 statistically-most-concerning conjunctions over the last year in LEO so they are four times less likely to be involved in a high-risk event than an average object in LEO. In addition, the PoC for a reported conjunction with any operational satellite (i.e., all OPL-ALL) might actually be smaller than depicted if onboard high accuracy ephemeris were used by the operator in determining a position covariance applied to the PoC calculation.

In examining the contribution of the Top 50 objects identified in 2019 [3], Figure 9 plots the data for the 5,934 conjunctions in the past year involving any of these 50 objects. First, 0.30% of the population (i.e., 50 out of 16,852 objects in LEO) accounted for 0.78% of the events which makes them 2.6 times more likely to be involved in a high-risk conjunction than the statistical average. Not surprisingly, the object that showed up the most times in conjunction events was an SL-16 R/B (SSN# 17974), which appeared 201 times. Examining the conjunction events in Figure 9, an SL-16 R/B appeared over 25% of the time while SL-8 R/Bs appeared 5% of the time. In aggregating the debris-generating potential from these 5,934 conjunctions, seven out of the top 10 objects were SL-16 R/Bs. Only one new object (not in the Top 50 list) contributed significantly in this subset of the high-risk encounters; a debris fragment from Cosmos 1275 was the 25th most likely to contribute to debris-generating events in LEO in this limited calculation.

In considering this analysis, it appeared that it might be useful to use all ~760,000 conjunctions to determine a "New Top 10" statistically-most-concerning objects to compare with the "Top 50 objects" from 2019. However, there were many occurrences where a single high-risk conjunction skewed the results based on that single event. As a result, it was decided that for the creation of the "New Top 10" objects list, the highest risk event for each object was omitted to soften the effects of a single encounter dominating the results. The "New Top 10 objects" are included in Appendix B. The following observations stem from this new list:

- All of the New Top 10 objects are of Russian origin, with an average time on orbit of 30 years. The most recent object was launched in 2007 and the oldest object was launched in 1982.
- The list includes six SL-16 R/Bs included in the original Top 50 (SSN#s: 19650, 22285, 23705, 26070, 23088, and 31793) that all reside between 830 and 850 km, reinforcing that particular altitude region is a prime candidate for remediation. These top six SL-16 R/Bs had an average of 160 conjunction events over the last year.
- While this is not a large list of objects, it is interesting to note that the primary objects are typically very old while the secondary objects are generally deployed or created much more recently. This mixing of the old, abandoned objects with new objects highlights the interdependency of debris remediation and debris mitigation; the less seriously we take debris mitigation the more debris remediation will be required.
- As stated in previous analyses, looking at highly coupled objects might identify uniquely efficient and effective remediation options whereby the removal of one object would cause another high priority object to

drop significantly in debris-generating potential. In this case, the two SL-16 R/Bs 23705 and 26070 are tightly coupled so removing one would likely cause the other's debris-generating potential to drop.

- While all of the Top 10 objects are Russian intact derelicts, the most coupled secondary objects are primarily Chinese and American. We examined all of the SL-16 RBs and the most coupled objects for 18 of the 20 SL-16 R/Bs were either Fengyun 1C debris or American debris (from NOAA 16, DMSP 5D-2 F13, and Thor Agena R/B). This observation highlights the global nature of the debris problem; it is clear that all major spacefaring countries have contributed to the current tenuous situation.
- The remaining four intact derelicts in the list reside at 330, 495, 530, and 545 km, respectively. Figure 5 highlights a local maximum around 330 km that seemed odd at first glance, but, on further investigation, Cosmos 1437 had 774 conjunctions over the last year as it decayed down to 330 km, enough to land it in the Top 10 list. The vast majority of the Cosmos 1437 conjunctions were with Starlink satellites. Clearly, an object at 330 km is not a candidate for remediation. This highlights that intact derelict objects that have been left to slowly decay can create a potentially significant collision avoidance burden on operational satellites.

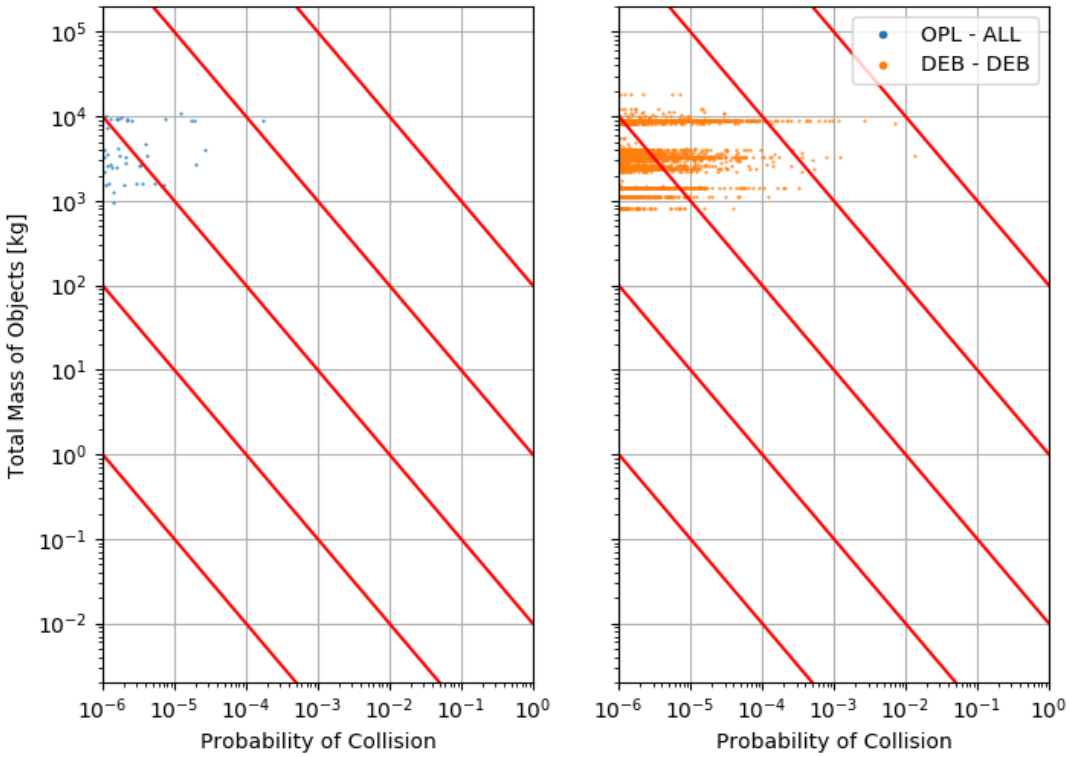

Fig. 9. The LCRC depicting only events that included the Top 50 objects shows that they clearly contribute to the highest-risk encounters.

3. ORBITAL CAPACITY METRIC

Several initiatives for quantifying the environmental impact of space missions, the sustainability of space activities and the capacity of Earth orbital regions, are under development (e.g., [6, 7]). One such initiative is the Space Sustainability Rating (SSR), developed by the World Economic Forum's Global Future Council on Space Technologies [8]. In general, these initiatives – including the SSR – produce composite indicators of the environmental 'footprint' represented by a space mission over its entire orbital lifetime, which can then be integrated over all space missions to gain an understanding of total orbital capacity. They incorporate assessments of collision

risk and adherence to Inter-Agency Space Debris Coordination Committee (IADC) Space Debris Mitigation Guidelines [9].

In contrast to these recent initiatives, Kessler and Anz-Meador developed a simple stability model [10] to estimate a value that can be likened to orbital capacity – the critical number of intact objects required to produce a "runaway" environment (the "Kessler Syndrome"). Their stability model was based solely on the rate at which objects pass through points in space due to atmospheric drag, thereby removing the need for a complex environment model or long-term predictions of the evolution of the orbital object population. The evolution of the orbital object population has an infinite number of trajectories that would overwhelm even the most powerful predictive model. As such, the rate-based approach taken by Kessler and Anz-Meador provides a way to understand what our present use of space might mean for future generations. As Lewis [11] argued, "As a starting point, we need to gain an understanding of the inheritance that the present generation will leave for all future generations of humanity. Rather than trying to predict the future, we must instead empathize with the future generations of space users and look back with that new awareness".

Consequently, we adopt a rate-based approach, similar to Kessler and Anz-Meador, to define the orbital capacity. Our approach is based upon a simple systems model of the orbital object population. In this system, the number of orbital objects represents the stock (Fig. 10). There are two inflows – objects added through new launch activity or explosions, and objects added due to collisions. The latter is a reinforcing feedback which depends on the number of objects in the population. There is one outflow, atmospheric decay, which is a balancing feedback that also depends on the number of objects in the population. In the future, active debris removal will hopefully provide another form of removal.

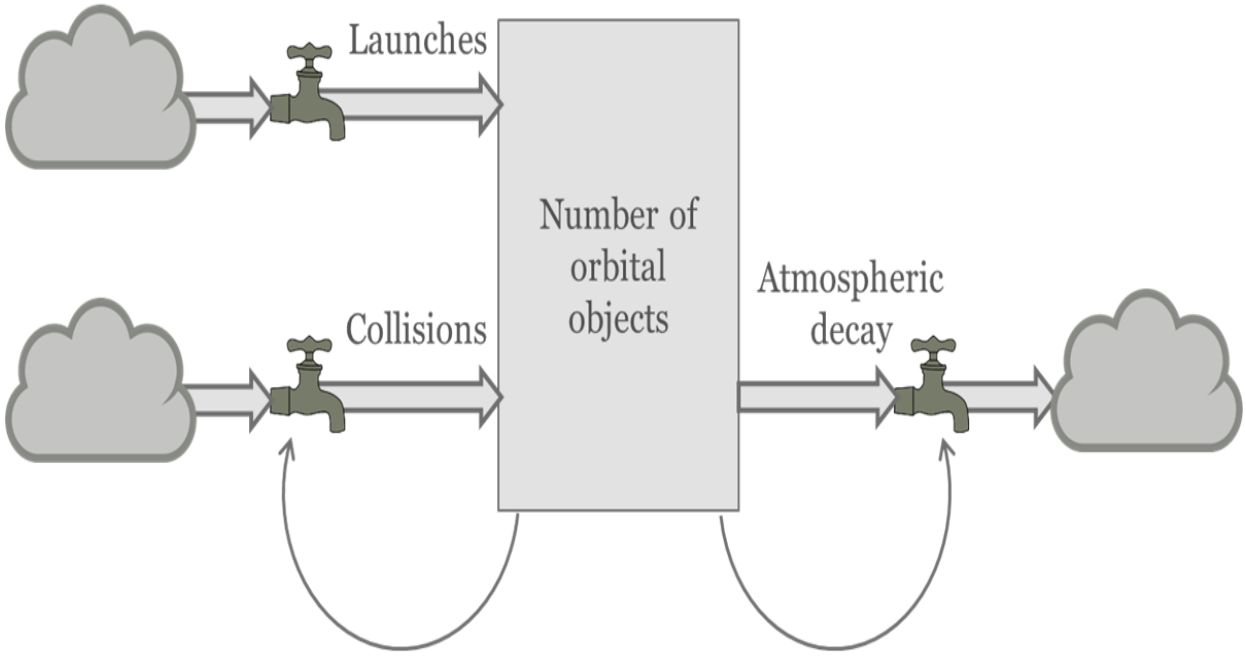

Fig. 10. Representation of the orbital object population system.

This simple systems model has been implemented in the past as a "Particles in a Box" (PIB) model with an ordinary differential equation (ODE) describing the flows [12]:

$$\frac{dN}{dt} = A - BN + CN^2 \tag{1}$$

where N is the number of objects in the population, A is the combined launch and explosion rate (i.e., the average number of orbital objects added each year by launch activity and explosions), BN is the re-entry rate (i.e., the

average number of objects leaving the "box" each year due to atmospheric decay) and CN^2 is the rate at which objects are added by collisions. Here the "box" represents the spherical shell around the Earth, extending from a height of 200 km to a height of 2000 km (i.e., the LEO region). The equilibrium populations are found easily from the roots of Eq. 1, using the quadratic formula,

$$N_{EQ} = \frac{B \pm \sqrt{B^2 - 4AC}}{2C} \tag{2}$$

Where the maximum value of the equilibrium population, N_{EQ}, is equivalent to the orbital capacity, as values of N greater than this will result in unconstrained, exponential population growth. Although this model is an obvious approximation of the real orbital object population system, it is simple and transparent, and can be readily extended to include multiple "boxes". For example, if two altitude regions are used to represent LEO (e.g., 200-1000 km and 1000-2000 km) then two ODEs will describe the population behavior:

$$\frac{dN_1}{dt} = A_1 - B_1 N_1 + C_1 N_1^2 + B_2 N_2 \tag{3}$$

$$\frac{dN_2}{dt} = A_2 - B_2 N_2 + C_2 N_2^2 \tag{4}$$

with objects from the higher altitude region decaying due to atmospheric drag into the lower altitude region (represented by the $+B_2 N_2$ term in the first ODE in Eq. 3). An assumption is that no objects decay into the higher altitude region from orbital regions below. The equilibrium populations for each "box" can again be found using the quadratic formula:

$$N_{EQ1} = \frac{B_1 \pm \sqrt{{B_1}^2 - 4(A_1 + B_2 N_2)C_1}}{2C_1} \tag{5}$$

$$N_{EQ2} = \frac{B_2 \pm \sqrt{{B_2}^2 - 4A_2 C_2}}{2C_2} \tag{6}$$

For each "box" there are three parameters that need to be determined, A, B, and C. To better understand the orbital capacity, we consider a scenario for which there are no launches and no explosions (i.e., $A = 0$). In other words, given the current orbital object population, will it increase due to random collisions alone? The parameter B in Eq. 1 is simply the reciprocal of the average time taken for orbital objects to decay out of the "box" – the orbital lifetime – which can be estimated using an atmospheric model and, for relatively long lifetimes, is proportional to the ballistic coefficient:

$$\beta = \frac{M}{SC_D} \tag{7}$$

where M is the object's mass, S is the object's cross-sectional area, and C_D is the drag coefficient. For an object with an area-to-mass ratio of 0.01 m^2/kg moving in a circular orbit through an atmosphere with exospheric temperature of 900°K (the average over a solar cycle), Figure 11 provides estimates of the orbital lifetime associated with different altitudes in LEO (based on predictions by King-Hele [13], using the COSPAR International Reference Atmosphere (CIRA) 1972).

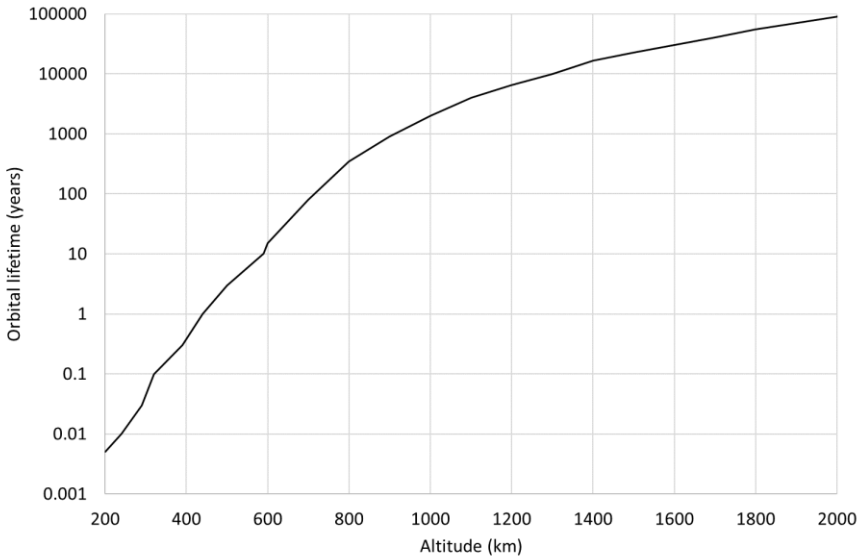

Fig. 11. Estimates of the orbital lifetime vs. altitude for an object with an area-to-mass ratio of 0.01 m^2/kg in a circular orbit, based on predictions made by King-Hele [13] using the CIRA-72 atmospheric model.

The parameter C, in Eq. 1, determines the rate at which collisions occur. If we have two identical, uniformly randomly distributed objects moving within a "box", then in one unit of time, the number of collisions, n, between the two objects is:

$$n = \frac{\sigma v}{V} \tag{8}$$

where σ is the combined cross-sectional area, v is the relative velocity between the two objects, and V is the volume of the spherical shell defined by the upper and lower altitude limits. If the objects are assumed to be spherical and identical, then the combined cross-sectional area is:

$$\sigma = 4S \tag{9}$$

In one year (which is the unit of time used for this PIB model) there would be $n \times \tau_Y$ collisions, where τ_Y is the number of seconds in one year. If we have N objects in the box, then the number of possible encounters between pairs of objects is $\frac{1}{2}N(N-1)$, but, if N is large, this can be approximated by $\frac{1}{2}N^2$ without significant error.

From [14], the number of fragments, F, of size L or larger generated by each collision is:

$$F = 0.1M^{0.75}L^{-1.71} \tag{10}$$

Hence, the expected rate at which new objects are added to the orbital population due to collisions in a "box" containing N objects is:

$$\frac{1}{2}nFN^2 \tag{11}$$

per year. By equating this to the ODE in Eq. 1, the parameter C is found to be:

$$C = \frac{1}{2}nF \tag{12}$$

Finally, and after some algebra, the maximum value of the equilibrium population, N_{EQ}, at any altitude for this PIB model (i.e., the orbital capacity) is found to be proportional to $S^{-1.75}$.

For this PIB model, the LEO region was divided into 14 shells, or "boxes" (in km), with the orbital object population dynamics in each described using an ODE of the form shown in Eq. 3[1]: 200-250, 250-300, 300-350, 350-400, 400-450, 450-500, 500-550, 550-650, 650-750, 750-850, 850-1000, 1000-1200, 1200-1400, 1400-2000. Objects in each box were assumed to be identical, spherical, and with an area-to-mass ratio of 0.01 m^2/kg. For each box, the parameter B was estimated using the orbital lifetime values from Fig. 11 based on an object located in the middle of the "box". The parameter C for each box was computed from Eq. 12, assuming $S = 1$ m^2 and $v = 11$ km/s. The use of $S = 1$ m^2 enables the orbital capacity results to be scaled for different object areas.

Fig. 12 gives the orbital capacity at different altitudes in LEO and for different object cross-sectional areas, in terms of the equilibrium number of orbital objects computed using the PIB model described above. For example, the orbital capacity for objects with cross-sectional area $S = 4$ m^2 at 700 km altitude is approximately 350 objects. In other words, exceeding this number would result in unconstrained, exponential population growth, according to the PIB model. The results also indicate that the orbital capacity may be lower than 10 objects at altitudes above 800 km, or lower than 1 object at altitudes above 1200 km. While a capacity of one derelict object may seem odd, it accentuates the effect of low atmospheric drag on the dynamics of the debris population in LEO. Going beyond capacity indicates the physical situation that will lead to an unstable population in the future through collisional encounters.

However, it should be noted that our analysis of the current LeoLabs catalog provides some grounding information about the relevance of these values. By considering only the massive derelicts (i.e., nonoperational payloads and rocket bodies) in LEO, the table below highlights the precarious position in LEO from the perspective of debris-generating potential for objects that are not capable of avoiding collisions. Operational satellites are ignored for this quick look, as many of them can avoid collisions with trackable objects, so will likely not drive debris generation in LEO while active. The thousands of debris fragments are also not considered as they contribute very little mass to the debris generation process. Neglecting both of these populations makes this assessment conservative – the probability of collision breakups adding to the rapid growth of the cataloged population is likely worse than our model predicts.

It is clear from comparing the values in Table 1 to the results in Fig. 12 that there are many altitude regions in LEO that have exceeded the point of imminent debris growth, even without any additional objects being added. For example, from Tab 1., the orbital capacity is exceeded above 750 km, while it is marginal between 550 and 750 km.

Tab.1 Empirical values for massive derelict number, mass, total area, and average area for LEO.

Altitude Range (km)	200-250	250-300	300-350	350-400	400-450	450-500	500-550	550-650	650-750	750-850	850-1000	1000-1200	1200-1400	1400-2000
Number	2	6	13	22	100	175	144	293	219	399	496	281	160	747
Average Area (m^2)	2	3	3	5	3	3	4	9	7	12	11	7	5	4
Exceeds capacity (Fig. 12)	no	no	no	no	no	no	no	close	close	YES	YES	YES	YES	YES

[1] Except for the 1400-2000 km "box", where the orbital object population dynamics were described using Eq. 4, based on the assumption that the orbital lifetimes for objects above 2000 km are essentially infinite.

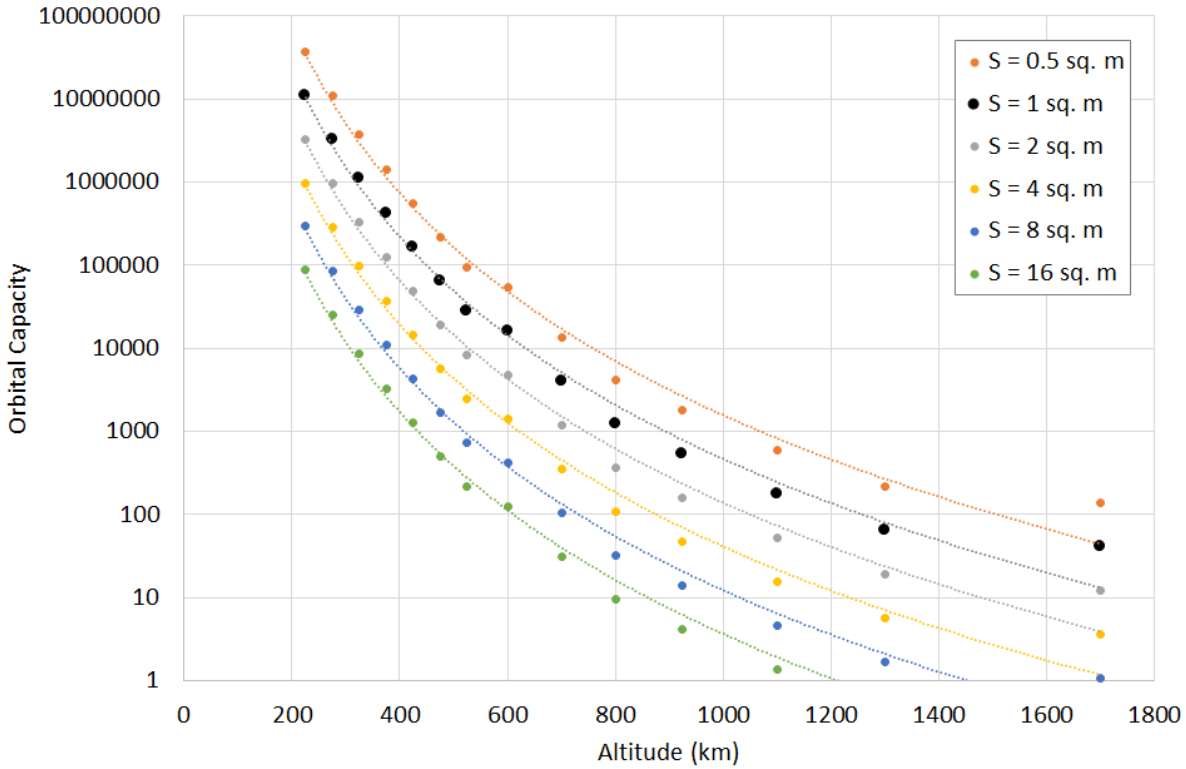

Fig. 12. Orbital capacity at different altitudes in LEO for objects with an area-to-mass ratio of 0.01 m^2/kg but varying cross-sectional area. Dashed lines are trendlines corresponding to Eq. 13.

Based on the PIB results, the orbital capacity for objects with an area-to-mass ratio of 0.01 m^2/kg can be approximated directly using the function:

$$N_{EQ} = 6.3330 \times 10^{22} h^{-6.7114} S^{-1.75} \tag{13}$$

where h is the altitude in km.

Considering the rates of change of the orbital object population (Fig. 13 and 14) gives greater insight into the population dynamics. For example, the population at altitudes below 500 km tends to have relatively large – though negative – rates of change, suggesting this is a low-risk environment. In contrast, the population at altitudes between 1400 and 2000 km would experience growth even for very small numbers of objects, but at a relatively low growth rate.

The effect of the large volume of this LEO region on the collision rate counteracts the effects of the very long orbital lifetimes. If the orbital capacity at altitudes 650-850 km were to be exceeded, this region would experience the greatest growth rate, unless a large number of objects (greater than the orbital capacity) were to populate the 500-550 km region. In that case, this low-altitude region would experience unconstrained, exponential growth at a rate exceeding any other in LEO, driven by the smaller volume and the weaker effects of atmospheric drag. Finally, the regions between 1000 and 1200 km and between 1200 and 1400 km tend to experience the same, relatively moderate, but positive rate of change, even for low numbers of objects. This region is therefore also one of concern, despite its relatively low current utilization [15].

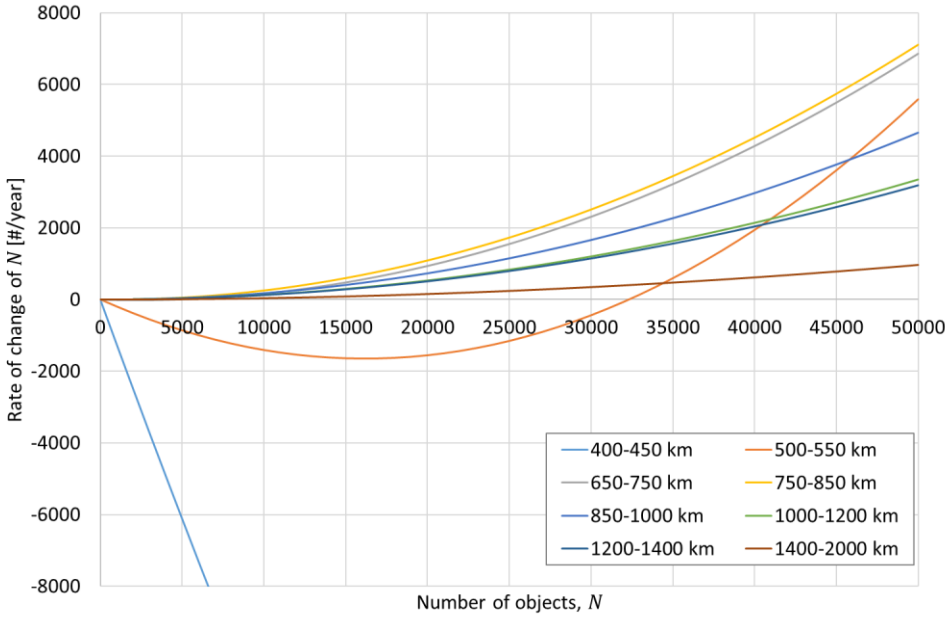

Fig. 13. Rate of change of the orbital object population ($S = 1$ m^2) predicted by the PIB orbital capacity model for population sizes up to 50,000 at different altitudes in LEO.

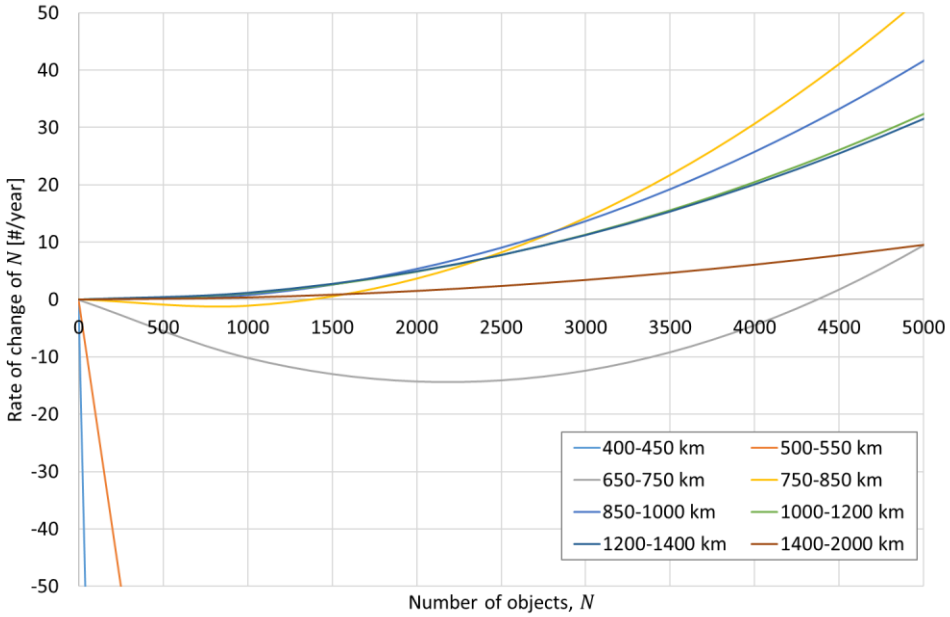

Fig. 14. Rate of change of the orbital object population ($S = 1$ m^2) predicted by the PIB model for population sizes up to 5000 at different altitudes in LEO.

The PIB orbital capacity model is simple and offers transparency. However, it is based on assumptions that are not fully representative of the physical reality. In particular, the model assumes that all objects, including fragments generated by collisions, are identical in size, shape, and mass, and move along circular orbits. Fragments will be smaller in size and mass than intact objects, will have different area-to-mass ratios, and will likely occupy eccentric orbits. Similarly, intact objects in LEO are diverse, with masses ranging from approximately 1 kg (CubeSats) to more than 10,000 kg (the Hubble Space Telescope). Nonetheless, the insights offered by the PIB model are consistent with those reported using substantially more complex models (e.g. [2]) and emphasize concerns about the orbital capacity at most altitudes in LEO, especially in relation to large, massive intact objects.

4. CONCLUDING REMARKS

From this data, several key observations can be made:

- **The greatest risk to space operations assurance in LEO is not posed by operational satellites and constellations but rather by thousands of massive intact derelict objects (defunct payloads and abandoned rocket bodies).** More pointedly, debris-on-debris collisions (where debris is the sum of fragments and derelict hardware) contribute twice the debris-generating potential than the risk posed by conjunctions between operational satellites and all resident space objects. The debris-generating potential of resident space objects is determined by the statistically-most-concerning conjunctions calculated by multiplying the probability of collision by the mass involved in the encounter (i.e., consequence). Tens of thousands of low probability and low consequence conjunction events (such as encounters with 1 km miss distances) are both statistically insignificant and operationally irrelevant.

- **As a result, the future safety of LEO satellites is more dependent on debris remediation efforts than space traffic management**. For reference, the total mass of the all Starlink satellites (at or below ~515 km and with robust collision avoidance capability) contains less mass then the 290 SL-8 R/Bs abandoned largely between 775 to 1200 km (i.e., will stay in orbit for decades to centuries and have no intent or ability to avoid collisions). Similarly, the 20 SL-16 R/Bs (abandoned largely at 830 to 850 km) amount to over half of the Starlink constellation mass. In addition, Starlink satellites comprise ~10% of the total LEO population but account for only 2.5% of the objects in the top 200 conjunctions driving debris-generating potential in LEO; so, as a constellation they pose a factor of four smaller collision hazard than an average object in LEO.

- **The large number of massive Russian derelict objects are the key population component that will likely generate large amounts of debris in the future, however, their debris-generating potential is largely driven by interactions with Chinese and American debris fragments and derelicts; this is a uniquely ironic collaborative effort.** The "new Top 10 statistically-most-concerning objects in LEO" list derived from the analysis of the ~760,000 conjunctions **reinforces the concern with SL-16 R/Bs**; six of the ten objects are SL-16 R/Bs in the 830 to 850 km altitude range.

- **The 775 to 850 km altitude range continues to be the region in LEO that is most concerning in terms of imminent debris generating events followed closely by the ~975 km and ~1,500 km altitudes**. The 775 to 850 km band is primarily driven by the 18 SL-16 R/Bs in this region spread between 830 to 850 km. **New capacity modeling of LEO also reinforced the concern with these regions leading to the determination that the orbital capacity is exceeded above 750 km** and is marginal between 550 to 750 km. The only regions that have not exceeded their orbital capacity is below 550 km which is largely driven by the cleansing effects of atmospheric drag not allowing the accumulation of debris and the fact that operational payloads at these altitudes largely have robust, active collision avoidance capability.

5. REFERENCES

[1] McKnight, D., Stevenson, M., Kunstadter, C., and Arora, R., Updating the Massive Collision Monitoring Activity – Creating a LEO Collision Risk Continuum, European Conference on Space Debris, April 2020.

[2] Lewis, H.G. (2020). Understanding long-term orbital debris population dynamics, J. Space Safety Eng. 7 (3), 164-170.

[3] McKnight, et al, "Identifying the 50 Statistically-Most-Concerning Derelict Objects in LEO," 71st International Astronautical Congress (IAC) – The CyberSpace Edition, Dubai, UAE, October 2020.

[4] Pardini, C. and Anselmo, L., EVALUATING THE ENVIRONMENTAL CRITICALITY OF MASSIVE OBJECTS IN LEO FOR DEBRIS MITIGATION AND REMEDIATION, *Acta Astronautica* **145** (2018) 51−75 [DOI: 10.1016/j.actaastro.2018.01.028]

[5] Rossi A., Valsecchi G.B., Alessi E. M, (2015). The Criticality of Spacecraft Index, *Advances in Space Research*, 56(3), 449–460.

[6] Letizia, F., Lemmens, S., and Krag, H. (2020). Environment capacity as an early mission design driver. Acta Astronautica, 173 (2020), 320-332.

[7] Maury, T., Loubet, P., Trisolini, M., Gallice, A., Sonnemann, G., and Colombo, C. (2019). Assessing the impact of space debris on orbital resource in life cycle assessment: a proposed method and case study. Science of the Total Environment, 667 (2019), 780-791.

[8] Rathnasabapathy, M. et al. (2020). Space Sustainability Rating: Designing a Composite Indicator to Incentivize Satellite Operators to Pursue Long-Term Sustainability of the Space Environment. 71st Int. Astronautical Congress CyberSpace Edition. IAC-20-E9.1-A6.8.6.

[9] Inter-Agency Space Debris Coordination Committee. (2021). IADC Space Debris Mitigation Guidelines. IADC-02-01. Rev. 3 (June 2021).

[10] Kessler, D.J., and Anz-Meador, P.D. (2001). Critical number of spacecraft in low earth orbit: using satellite fragmentation data to evaluate the stability of the orbital debris environment. 3rd European Conference on Space Debris, April 2001.

[11] Lewis, H.G., and Marsh, N. (2021). Deep time analysis of space debris and space sustainability. 8th European Conference on Space Debris, April 2021.

[12] Talent, D.L. (1992). Analytic model for orbital debris environmental management. Journal of Spacecraft and Rockets, 29 (4), 508-513.

[13] King-Hele D., (1987). Satellite Orbits in an Atmosphere: Theory and Applications, Blackie.

[14] Johnson, N.L., Krisko, P.H., Liou, J.-C., and Anz-Meador, P.D. (2001). NASA's new breakup model of EVOLVE 4.0. Advances in Space Research, 28 (9), 1377-1384.

[15] European Space Agency. (2021). ESA's annual space environment report. Revision 5 (May 2021).

Appendix A. Top 30 Riskiest Conjunctions, 1 July 2020 to 30 June 2021

"Risk" [kg]	LeoLabs IDs		SSN IDs		Names	
255.00	881	7321	19826	36123	COSMOS 2004	CZ-4C R/B
56.90	335	2235	27386	19365	ENVISAT	DELTA 1 DEB
46.70	1813	9020	17973	7218	COSMOS 1844	OPS 8579 (DMSP 5B F5)
34.10	4684	4696	13589	16594	COSMOS 1410	SL-14 R/B
29.50	7059	4573	16953	8344	SL-8 R/B	SL-8 R/B
23.50	11965	12069	22803	34796	SL-16 R/B	COSMOS 2251 DEB
16.70	2936	205	20805	22335	SL-8 R/B	SL-16 DEB
16.10	166091	11430	44487	17911	OBJECT B	COSMOS 1842
14.00	5335	9910	39627	3504	CZ-2C DEB	COSMOS 249
11.80	4282	6411	22565	20867	COSMOS 2237	CZ-4 DEB
11.40	2738	1214	40287	11113	CZ-2C R/B	SL-8 DEB
10.40	4373	6746	17590	34019	SL-16 R/B	COSMOS 2251 DEB
9.85	363	12880	29228	3757	RESURS DK-1	COSMOS 249 DEB
9.22	5136	11618	12443	10820	SL-8 R/B	OPS 6182 (DMSP 5D-1 F3)
8.51	4148	60201	25407	39633	SL-16 R/B	DMSP 5D-3 F19 DEB
8.00	3928	48239	19210	43843	COSMOS 1953	OBJECT N
7.93	16858	61409	41858	43931	CZ-2D R/B	IRIDIUM 167
7.61	2027	9703	22566	323	SL-16 R/B	THOR ABLESTAR DEB
7.18	5577	47848	23317	43783	OKEAN 4	KAZSTSAT
7.03	1839	5711	410	7009	THOR ABLESTR DEB	SL-8 R/B
6.92	945	4219	22307	4636	COSMOS 2230	THORAD AGENA D DEB
6.79	9709	10180	10120	24903	COSMOS 923	IRIDIUM 26
6.65	12948	529	18215	33320	SL-14 R/B	HJ-1A
6.60	4068	6179	19650	34613	SL-16 R/B	COSMOS 2251 DEB
6.53	4334	12911	37673	4311	SAC-D (AQUARIUS)	THORAD AGENA D DEB
6.52	2603	102916	25077	7816	IRIDIUM 42	OPS 6226
6.23	7700	4899	22284	39265	COSMOS 2227	CASSIOPE
5.83	5438	3981	18748	15889	COSMOS 1908	COSMOS 1666
5.48	4803	3406	16182	30209	SL-16 R/B	FENGYUN 1C DEB
5.28	613	4059	38707	14372	KANOPUS-V 1	COSMOS 1500
5.24	3448	1312	39154	32783	CZ-2D R/B	CARTOSAT 2A
5.21	167	7618	28057	39670	CBERS 2	COSMOS 1867 COOLANT
5.06	7191	195147	15944	44810	COSMOS 1674	FLOCK 4P 12
4.93	342	19744	14699	43103	COSMOS 1536	CZ-2D DEB
4.78	367	5970	8646	11804	SL-8 R/B	SL-8 R/B
4.71	4198	2972	33591	4158	NOAA 19	THORAD AGENA D DEB
4.69	6863	5005	19211	24926	SL-14 R/B	DUMMY MASS 2
4.62	805	1342	37215	27160	CZ-4C R/B	PSLV DEB
4.48	3152	4278	8293	31311	METEOR 1-22	FENGYUN 1C DEB
4.47	2330	60196	24297	28054	COSMOS 2333	DMSP 5D-3 F16 (USA 172)
4.45	3129	4161	20853	2802	CZ-4 DEB	SL-8 R/B
4.40	9442	17152	25985	41917	ORBCOMM FM 35	IRIDIUM 106
4.26	10016	7226	20509	17067	SL-8 R/B	SL-8 R/B
4.14	1943	4042	22080	13736	COSMOS 2208	OPS 9845 (DMSP 5D-2 F6)
4.08	4068	688	19650	22432	SL-16 R/B	SL-16 DEB
4.08	12666	7213	20625	41080	SL-16 R/B	NOAA 16 DEB
4.05	3586	3351	27561	25736	RUBIN 3/SL-8	MUBLCOM
4.05	4790	170	15099	15780	METEOR 2-11	COSMOS 1275 DEB
4.02	3622	12006	23087	8954	COSMOS 2278	DELTA 1 DEB
3.95	1022	4578	14033	39428	SL-14 R/B	DELFI-N3XT

Appendix B. “New Top 10” Statistically-Most-Concerning Objects in LEO, 1 July 2020 to 30 June 2021

Rank	# of Events	Launch Year	LeoLabs#	SSN IDs#	Object	Perigee/ Apogee	Inclination	Most Coupled Secondary Object
1	169	1988	L4068	19650	SL-16 R/B	830/849	71	Fengyun 1C debris SSN# 37917
2	176	1992	L10362	22285	SL-16 R/B	838/846	71	NOAA 16 debris SSN# 41422
3	160	1995	L1978	23705	SL-16 R/B	834/850	71	SL-16 R/B SSN# 26070
4	174	2000	L1642	26070	SL-16 R/B	828/853	71	SL-16 R/B SSN# 23705
5	156	1994	L10578	23088	SL-16 R/B	839/847	71	DMSP 5D-2 F13 debris SSN# 40398
6	506	1988	L1996	19274	OKEAN 1	538/554	83	Starlink 1451 SSN# 45688
7	774	1983	L2492	13770	Cosmos 1437	330/332	81	Starlink 1431 SSN# 47839
8	171	2007	L5162	31793	SL-16 R/B	842/846	71	Fengyun 1C debris SSN# 30453
9	810	1981	L5207	12586	SL-3 R/B	519/546	98	Starlink 1272 SSN# 45386
10	138	1982	L11667	13271	Cosmos 1378	489/500	82	Gaofen 11 SSN# 43585